Exciton Dynamics in soluble Poly(*p*-phenylene-vinylene): Towards an Ultrafast Excitonic Switch

S. V. Frolov, M. Liess, P. A. Lane, W. Gellermann, and Z. V. Vardeny
University of Utah, Physics Department, Salt Lake City, Utah 84112

M. Ozaki and K. Yoshino
Electronic Engineering Department, Osaka University, Yamada-Oka 2-1, Suita, Japan
(Received 8 November 1996)

We have applied a variety of ps transient and cw optical techniques to elucidate the dynamics, absorption, and emission properties of excitons in soluble derivatives of poly(*p*-phenylene vinylene) neat films and dilute solutions. We found that the photogenerated singlet excitons in both films and solutions are characterized by strong stimulated emission and *two* photoinduced absorption bands. We demonstrate that these bands can be used to form an ultrafast optical switch in the near IR spectral range with variable switching times. [S0031-9007(97)03244-4]

PACS numbers: 78.45.+h, 71.35.Cc, 76.70.Hb, 78.47.+p

The most striking optical property of many π-conjugated conducting polymers is a bright photoluminescence (PL) band with high quantum efficiency, which can be chemically tuned to cover the complete visible spectral range [1]. Their application in optical emission devices such as light emitting diodes and, more recently, laser-active media has led to intensive investigations of conducting polymers, such as poly(*p*-phenylene-vinylene) (PPV) and its derivatives [2]. Attention has been focused on the properties of photogenerated excitons in neat films of these materials [3,4]. However, the exact spectral signatures of photoexcitations in PPV, i.e., singlet excitons, triplet excitons, and polaron pairs, have remained unclear so far because of their strong overlapping spectral features in the visible to near IR (NIR) spectral range [3].

In this Letter we have elucidated the dynamics, absorption, and emission properties of excitons in neat films and dilute solutions of PPV derivatives, using transient and cw photomodulation (PM) and PL measurements, photoinduced absorption (PA) detected magnetic resonance (PADMR) and electroabsorption (EA) spectroscopies. We show that the photogenerated singlet excitons are the primary excitations in both neat films and solutions. By applying a novel transient experimental technique involving three ps pulsed beams, we prove that the singlet excitons are characterized by a stimulated emission (SE) band at 2.2 eV accompanied by phonon replicas, and two PA bands at 0.9 and 1.5 eV, respectively. Making use of the fact that both the SE and PA bands are related to the same excitons, we demonstrate an ultrafast optical excitonic switch in the NIR spectral range.

Transient PM measurements were performed using the pump-and-probe correlation technique employing three lasers synchronously pumped by a mode-locked Nd:YAG laser: two dye lasers and a color center laser [5]. The pump photon energy was fixed at 2.2 eV, whereas the probe photon energy was varied between 0.76 and 0.86 eV, using the color center laser, and from 1.25 to 2.2 eV, using one of the dye lasers. We measured the changes ΔT in the probe transmission T using a fast acousto-optic modulation scheme, Si and Ge detectors, and a fast lock-in amplifier. The time resolution of the transient PM apparatus was 5–10 ps, as determined by a measurement of pump-probe cross correlation. The transient PL decays were measured with a streak camera having 10 ps time resolution in a synchroscan mode. The PM and PL measurements were conducted at low exciton densities, $N < 10^{17}$ cm^{-3}, to avoid significant exciton-exciton interactions; this low intensity also resulted in pump photobleaching efficiency of less than 0.1%.

A standard steady-state PM setup was used for the cw optical measurements [6]. The pump was a modulated beam from an Ar^+ laser and the probe was an incandescent lamp. For the PADMR spectra we measured the changes in PA induced by a modulated μ-wave field (at 3 GHz) in resonance with the Zeeman split spin triplet sublevels in magnetic field H [6]. A similar setup was also used for the EA measurements [7], where ΔT is caused by a modulated electric field in the polymer film, of order 10^5 V/cm.

We measured a variety of PPV soluble derivatives with very similar results. In this paper we concentrate on 2,5-dioctyloxy PPV (DOO-PPV) films and dilute solutions; DOO-PPV backbone structure is given in Fig. 1(b), inset. Fresh DOO-PPV thin films were cast from chloroform solutions of 5% molar concentration onto quartz substrates; the films were constantly kept in vacuum.

The transient PM spectra of DOO-PPV films at room temperature, plotted as $-\Delta T/T$ from 0.75 to 2.2 eV, are shown in Fig. 1(a) for time delays $t = 0$ ps and 1.2 ns, respectively. Above $\hbar\omega = 1.7$ eV we measured $\Delta T > 0$; and since the ground state absorption onset is at 2.2 eV, this band is due to SE rather than photobleaching of the absorption [3,8]. This can be also inferred from the similarity of the SE and the PL spectra, both of which contain several phonon replicas at ~1.8, 1.98, and 2.15 eV, respectively [Fig. 1(a)]. Below $\hbar\omega = 1.7$ eV

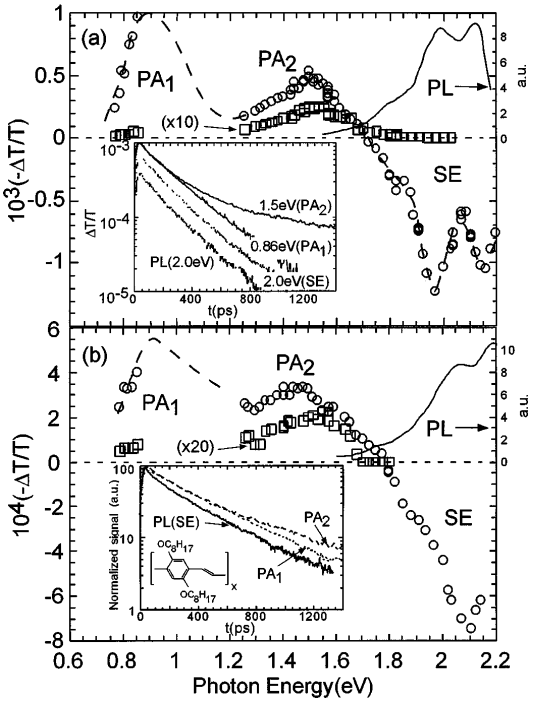

FIG. 1. Transient photomodulation spectra of DOO-PPV: (a) solid film at $t = 0$ ps (circles) and $t = 1.2$ ns ($\times 10$), (b) dilute solutions at $t = 0$ ps and $t = 2$ ns ($\times 20$). The dashed lines are to guide the eye. Various PA and SE bands are assigned. The PL spectra are also shown for comparison with the SE. Insets compare the PL and the various PM decay dynamics. The backbone structure of DOO-PPV is given in inset (b).

we observed two PA bands with $\Delta T < 0$, peaking at $\hbar\omega = 0.9$ eV (PA_1) [9] and 1.5 eV (PA_2), respectively. The decay dynamics of the SE, PA_1, and PA_2 bands are compared to that of the PL band in the inset of Fig. 1(a). Except for PA_2, all show a single exponential decay dynamics with lifetime $\tau_s = 240$ ps, which is equivalent to the decay of the photogenerated excitons density. PA_2 initially follows the same exponential decay dynamics up to ~300 ps, then it deviates and becomes much slower, dominating the PM spectrum at longer times. As seen in Fig. 1(a), the PM spectrum at $t = 1.2$ ns contains only a single asymmetric PA band, which is slightly blueshifted from PA_2, while PA_1 and SE are barely detectable at 1.2 ns.

We observed similar PM spectra in DOO-PPV dilute solutions, shown in Fig. 1(b). PA_1, PA_2, and SE can be again identified at the same probe photon energies as those in films. τ_s in solutions, however, is longer [~440 ps, Fig. 1(b), inset], and PA_2 deviates from a single exponential dynamics at much longer times (>1 ns). The primary excitations in DOO-PPV dilute solutions must be singlet excitons, since the polymer chains are isolated and hence, the possibility of exciton dissociation into polaron pairs is greatly reduced. Then from the similarity of the PM spectra and their decays in DOO-PPV films and dilute solutions seen in Figs. 1(a) and 1(b), we conclude that the primary excitations in DOO-PPV films are also singlet excitons [4,10]. The long excitonic lifetime and a corresponding high PL quantum efficiency [11] indicates that DOO-PPV is a high quality polymer material, which is very suitable for electro-optics and laser action applications [12].

The PM spectrum of excitons in DOO-PPV is schematically explained in Fig. 2(a), which shows the ground and excited electronic levels and their associated optical transitions in a configuration coordinate (Q) diagram [13]. The pump beam induces transitions from the ground state ($1A_g$) to the first allowed excitonic state ($1B_u$). Following a relatively small relaxation (~0.1 eV), SE (and PL) occurs between the relaxed $1B_u$ and $1A_g$. In addition to SE, PA from $1B_u$ to higher energy levels is induced for two even-parity states, namely, mA_g and kA_g [Fig. 2(a)]. In a related study in our group, these two A_g states have been directly measured by two-photon absorption spectroscopy [14]. We note that recent elegant theoretical calculations have identified mA_g and kA_g as charge transfer exciton and biexciton (bound state of two excitons), respectively [15], but their exact character cannot be inferred from our PM measurements.

The energy level diagram in Fig. 2(a) is substantiated by the EA spectrum measured on the same DOO-PPV films, as shown in Fig. 2(b). The EA spectrum is composed of a derivativelike feature with zero crossing at 2.25 eV, which is due to the quadratic Stark shift of the $1B_u$ exciton at this energy [7], and two positive bands at 3.0 and 3.5 eV, respectively. These bands are due to even parity states (mA_g and kA_g), which become

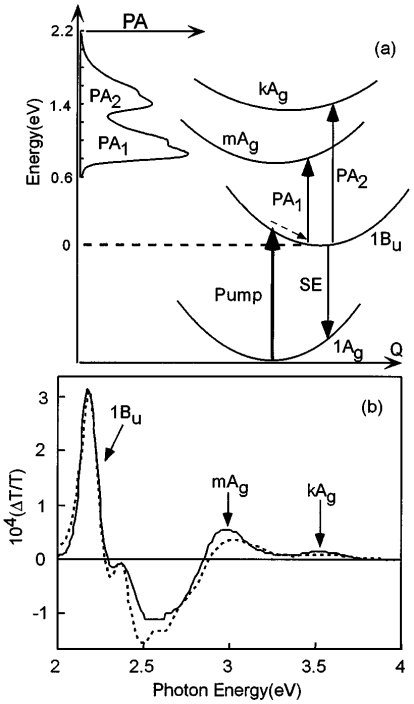

FIG. 2. (a) Configuration coordinate diagram of the exciton model and optical transitions in DOO-PPV. (b) The EA spectrum (solid line) and its fit (broken line).

partially allowed in EA due to symmetry breaking caused by the strong applied electric field F. We successfully simulated the EA spectrum [Fig. 2(b)] by calculating the imaginary part of the third order optical nonlinear susceptibility [13], $\mathrm{Im}[\chi^{(3)}(\omega; -\omega, 0, 0)]$, where $\Delta\alpha(\mathrm{EA}) \sim \mathrm{Im}(\chi^{(3)})F^2$. Calculations were done using summation over the states shown in Fig. 2(a), and their strongly coupled vibrations using appropriate Frank-Condon overlap integrals [13]. The fitting parameters were $1B_u$, mA_g, and kA_g energy levels, their dipole couplings and relative configuration coordinate displacements, ΔQ [16]; whereas the frequency of the strongest coupled C = C stretching mode (1600 cm^{-1}) was directly determined by Raman scattering. Using the fitting parameters of the EA spectrum, we were also able to calculate the PA spectrum from the relaxed $1B_u$ exciton to the mA_g and kA_g levels using the Huang-Rhys approximation [Fig. 2(a)]. The calculated spectrum [16] agrees very well with the experimental PA bands at $t = 0$ ps (Fig. 1) and thus validates our model.

The slower component of PA_2 deviates from the respective SE and PA_1 decays, which correspond to singlet excitons dynamics, $N(t)$ at about 300 ps in DOO-PPV films [Fig. 1(a), inset]. This slower PA component can be measured at 300 K by cw PM (Fig. 3) in more details; it shows a peak at 1.45 eV and the absence of a second correlated PA band at 0.8 eV. From its modulation frequency dependence, we estimate a corresponding lifetime of about 5 μsec. The spin signature related to this slow PA can be readily measured at low temperatures by PADMR [17]. The H-PADMR spectrum at the peak of the slow PA (1.45 eV in Fig. 3, inset) shows a single asymmetric band at 390 G, which corresponds to $\Delta m = \pm 2$ transitions between triplet sublevels at "half-field." This strongly suggests that the slow PA band is due to triplet excitons. In fact, the λ-PADMR spectrum at 390 G (dashed line in Fig. 3) fits very well both the transient ($t = 1.2$ ns) and cw PA bands [Fig. 1(a) and Fig. 3, respectively]. Exciton dissociation into polaron pairs would give a strong $S = \frac{1}{2}$ H-PADMR signal at 1068 G [6], in contrast to our observations. We therefore conclude that the slower PA_2 dynamics are due to intersystem crossing (ISC) from singlet to triplet excitons having a much longer lifetime.

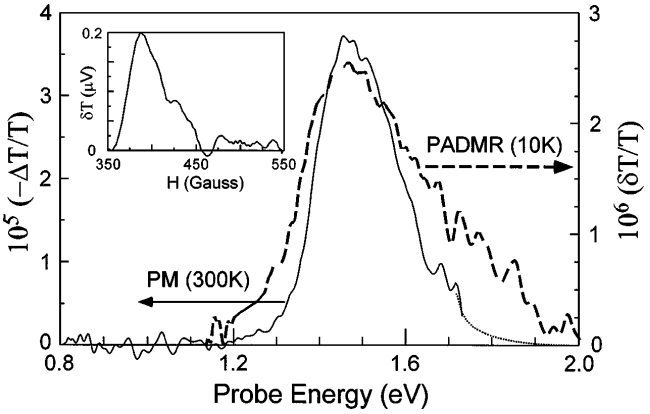

FIG. 3. CW PA spectrum at 300 K (solid line) compared with PADMR triplet spectrum at 10 K (broken line). The inset shows the H-PADMR spectrum at 1.45 eV.

The ISC rate in π-conjugated polymers has been generally assumed to be low [3]. However, it can be enhanced in polymer films due to the presence of paramagnetic (spin 1) O_2 molecules [18]. Assuming that PA_2 is composed of contributions from both singlet and triplet excitons, we calculate for ΔT at $\hbar\omega = 1.45$ eV,

$$\Delta T = c[e^{-t/\tau_s} + a(1 - e^{-t/\tau_s})], \qquad (1)$$

where a and c are constants. In Eq. (1), a is given by $\sigma_t\tau_s/\sigma_s\tau_{\mathrm{ISC}}$, where σ_s and σ_t are the optical cross sections of PA at 1.45 eV for singlet and triplet excitons, respectively, and τ_{ISC} is the ISC time. From the PA_2 dynamics [Fig. 1(a), inset] we found $a = 0.06$. Then from $\tau_s = 240$ ps we calculate $\tau_{\mathrm{ISC}} \sim 4$ ns, assuming $\sigma_s \sim \sigma_t$. The same analysis for PA_2 decay in DOO-PPV solutions gives $\tau_{\mathrm{ISC}} \sim 20$ ns. The slower ISC rate in solutions is consistent with the lower dissolved O_2 density.

In contrast to excitons in inorganic semiconductors with small binding energies, excitons in conducting polymers with relatively large binding energies [19] may be used to form optical switches and modulators in the NIR spectral range. This is demonstrated for the excitons in DOO-PPV, where SE and two associated PA bands are used to modulate the sample absorption in th NIR [5]. For these measurements we used three ps pulsed laser beams, as shown in Fig. 4(a), inset: (i) The pump beam at $\hbar\omega \geq 2.2$ eV is used to generate excitons at $t = 0$ ps, where the excitonic switch is turned on. (ii) The dump beam, which is tuned within the SE spectral range (in the polymer transparency region), is delayed in time by $t = t_1$. The radiative recombination of some of the photogenerated excitons is then stimulated by the dump pulse at $t = t_1$, thereby turning off the excitonic switch. (iii) The probe beam at $t = t_2$, which is tuned within PA_1 or PA_2 spectral ranges, is used to measure the resulting "pump-and-dump" transient PA.

In Figs. 4(a) and 4(b) we chose the pump at 2.2 eV, the dump at 2.0 eV, and the probe at 0.8 eV, respectively. The dump beam fluence was on the order of 10^{13} cm^{-2}. Figure 4(a) compares the respective transient decays of PA_1 with and without the dump pulse at $t_1 = 150$ ps; the difference, δT, in the PA decays is also shown. It is seen that the PA magnitude is reduced (or "switched off") at t_1 by about 20%. This switching effect is caused by the decrease in the singlet exciton population, δN, due to SE induced by the dump pulse at t_1. The reduced PA at $t > t_1$ continues to follow the same exponential decay as for $t < t_1$, since the recombination process is monomolecular in origin with no correlation among the photogenerated excitons. As seen in Fig. 4(a) this also leads to an exponential dynamics for $\delta T(t)$. In Fig. 4(b) we show $\delta T(t)$ decays for different "switch-off" times, t_1,

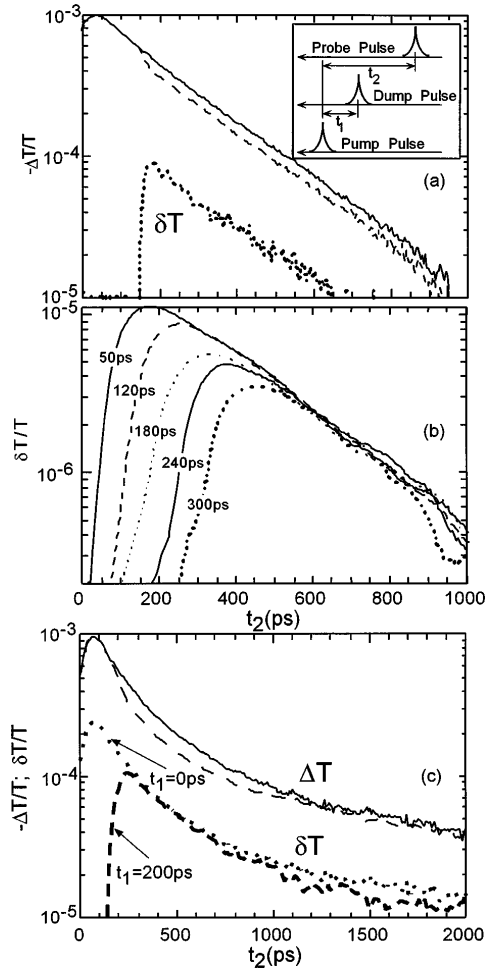

FIG. 4. Three beam transient PM measurements: (a) ΔT at PA_1 (0.8 eV) without dump (solid line), with dump at $t_1 = 150$ ps (broken line), and the difference δT (dotted line); the inset shows schematically the three beam experimental setup. (b) δT transients at PA_1 (0.8 eV) for various t_1 delays. (c) ΔT at PA_2 (1.5 eV) without dump (solid line) and with dump at $t_1 = 200$ ps (broken line); the lower curves show δT for $t_1 = 0$ ps (dotted) and $t_1 = 200$ ps (dashed).

in the range from 50 to 300 ps to demonstrate the variable switching time of the excitonic switch device. We note that all $\delta T(t)$ decays follow the same exponential form with lifetime τ_s, independent of t_1. This simple decay form can be readily explained by a SE process at $t = t_1$, since $\delta N(t_1)$ is proportional to $N(t_1)$, where $\delta N(t_1)$ is the number density of "dumped" excitons.

In Fig. 4(c) we also demonstrate the excitonic switch for PA_2. In this case we kept the pump and dump at 2.3 and 2.0 eV, respectively, and tuned the probe to 1.5 eV. Again we show PA_2 decays with and without the dump pulse at $t_1 = 200$ ps. It is seen that δT is formed at $t = t_1$, *providing direct evidence that PA_2 is also related to singlet radiative excitons,* similar to PA_1. Thus we can also use the excitonic switch in the far red optical range. We found, however, that in contrast to the switch at PA_1, δT decay in the PA_2 spectral range depends on t_1. At $t_1 = 0$ ps $\delta T(t)$ decays exactly as $\Delta T(t)$, as shown in Fig. 4(c). However, for $t_1 > 0$ $\delta T(t)$ deviates from $\Delta T(t)$ and the deviation increases with the switch-off time, t_1, as seen in Fig. 4(c) for δT at $t_1 = 0$ and 200 ps, respectively. The reason for this more complex behavior of δT at PA_2 is the mixed contributions to PA_2 at $t > 0$ ps from both singlet and triplet excitons. δT is caused by singlet exciton alone, since triplet excitons do not radiate and therefore cannot be influenced by the dump pulse via SE at 2.0 eV. Then, since the contribution of triplet excitons increases with t_1, the deviation of $\delta T(t)$ from $\Delta T(t)$ becomes more apparent at longer t_1.

In summary, we found that photogenerated singlet excitons in DOO-PPV films and dilute solutions have a strong SE in the visible, and two associated PA bands in the NIR spectral ranges. These bands can be used to form an ultrafast excitonic switch with variable switching times, providing direct evidence of the primary excitations in DOO-PPV. In addition, we determined the ISC time into the triplet manifold to be of order 5 ns and solved the puzzle regarding PA_2 at 1.5 eV [3]; we found that both singlet and triplet excitons strongly contribute to PA at 1.5 eV.

We acknowledge fruitful discussions with S. Mazumdar and L. Rothberg. The work at the University of Utah was supported in part by the DOE, FG-03-96-ER 45490 and ONR Grant No. N00014-94-1-0853.

[1] D. D. C. Bradley, Polym. Int. **26**, 3 (1991).
[2] For a review see *Proceedings of the International Conference on Synthetic Metals 96, Salt Lake City, Utah, 1996* [Synth. Met. **84** (1997)].
[3] M. Yan *et al.,* Phys. Rev. Lett. **72**, 1104 (1994).
[4] N. T. Harrison *et al.,* Phys. Rev. Lett. **77**, 1881 (1996).
[5] S. V. Frolov, Ph.D. thesis, University of Utah, 1996 (unpublished).
[6] X. Wei *et al.,* Phys. Rev. B **53**, 2187 (1996).
[7] S. A. Jeglinski *et al.,* Mol. Cryst. Liq. Cryst. **256**, 87 (1994).
[8] M. Yan *et al.,* Phys. Rev. Lett. **75**, 1992 (1995); W. Graupner *et al., ibid.* **76**, 847 (1996); J. W. Blatchford *et al., ibid.* **76**, 1513 (1996); T. Pauck *et al.,* Chem. Phys. Lett. **244**, 171 (1995).
[9] PA_1 peak is out of the measured spectral range and thus may be at 0.9–1.0 eV.
[10] J. M. Leng *et al.,* Phys. Rev. Lett. **72**, 156 (1994).
[11] I. D. W. Samuel *et al.,* Phys. Rev. B **52**, R11 573 (1995).
[12] S. V. Frolov *et al.,* Jpn. J. Appl. Phys. **35**, L1371 (1996).
[13] M. Liess *et al.,* In Ref. [2], p. 891.
[14] R. Meyer *et al.,* in Ref. [2], p. 549.
[15] M. Chandross *et al.,* in Ref. [2]; (to be published).
[16] From Ref. [13] the fitting parameters to the EA spectrum are $E_{1B_u} = 2.3$ eV, $E_{mA_g} = 3.0$ eV, $E_{kA_g} = 3.55$ eV, $\Delta Q_{1B_u} = 0.9$, $\Delta Q_{mA_g} = \Delta Q_{kA_g} = -0.9$.
[17] X. Wei *et al.,* Phys. Rev. Lett. **68**, 666 (1992).
[18] E. Frankevich *et al.,* Phys. Rev. B **53**, 4498 (1996).
[19] M. Chandross *et al.,* Phys. Rev. B **50**, 14 702 (1994).